

Entrapment and interaction of an air bubble with an oscillating cavitation bubble

Y. S. Kannan, Badarinath Karri* and Kirti Chandra Sahu†

Department of Mechanical and Aerospace Engineering,

Indian Institute of Technology Hyderabad, Kandi, Sangareddy 502 285, Telangana, India

†Department of Chemical Engineering, Indian Institute of Technology Hyderabad, Kandi, Sangareddy 502 285, Telangana, India

(Dated: April 5, 2018)

The mechanism of the formation of an air bubble due to an oscillating cavitation bubble in its vicinity is reported from an experimental study using high-speed imaging. The cavitation bubble is created close to the free surface of water using a low-voltage spark circuit comprising two copper electrodes in contact with each other. Before the bubble is created, a third copper wire is positioned in contact with the free surface of water close to the two crossing electrodes. Due to surface tension at the triple point (wire-water-air) interface, a small dip is observed in the free surface at the point where the wire is immersed. When the cavitation bubble is created, the bubble pushes at the dip while expanding and pulls at it while collapsing. The collapse phase leads to the entrapment of an air bubble at the wire immersion point. During this phase, the air bubble undergoes a ‘catapult’ effect, i.e., it expands to a maximum size and then collapses with a microjet at the free surface. To the best of our knowledge, this mechanism has not been reported so far. A parametric study is also conducted to understand the effects of wire orientation and bubble distance from the free surface.

It is well known that an oscillating non-equilibrium bubble in a non-uniform surrounding pressure field such as due to the presence of a free surface or a rigid boundary leads to the formation of a re-entrant jet in the bubble in its collapse phase. This re-entrant jet is directed away from free surface [1, 2] and towards rigid boundary [3, 4]. The collapse of the bubble is also accompanied by the formation of shock waves. In cases, where the bubble is created close to a free surface, there are also jets formed on the free surface [1, 2] in addition to the re-entrant jet in the bubble. Depending on the distance of the bubble from the free-surface, a variety of different jets have been observed such as water film, spraying water film, swallowed water spike, etc [5].

Researchers have also reported other means to create free surface jets. For example, Kian *et al.* [4] conducted experiments where they saw high speed jets at the meniscus inside a capillary tube caused by flow focusing at the meniscus due to a shock wave. Tagawa *et al.* [6] also reported a phenomenon where a laser induced bubble is created close to the meniscus in a capillary tube. They found that a shock wave is generated at the onset of bubble generation, and the interaction of this shock wave with the liquid meniscus lead to the generation of jets with velocities up to 850 m s^{-1} . Blake *et al.* [7] have performed experiments to understand the interaction of two oscillating bubbles near a solid boundary. They have concluded that the presence of a bubble near another bubble also effects the behavior of the bubble. Jungnickel *et al.* [8] have conducted experiments to study the interaction of two laser induced cavitation bubbles. They inferred that the dominant interaction mechanism between the bubbles is due to the mutual interaction between the bubbles. Pain *et al.* [9] conducted experiments

to illustrate the interaction of a stationary bubble with an oscillating bubble and found that this interaction leads to a jet in the stationary bubble with a velocity up to 250 m s^{-1} . Here, the stationary bubble was trapped inside a droplet before creating the oscillating bubble. The interaction of multiple oscillating bubbles are also studied by Fong *et al.* [10] and several complex phenomena such as bubble splitting and high-speed jetting inside one bubble caused by the collapse of a nearby bubble were investigated. Karri *et al.* [11, 12] reported experiments where a bubble was created below a hole in a plate which itself was placed near a free surface. This led to impinging jets at the free surface and spray formation because of the hole in the plate.

Recently, Avila *et al.* [13] used a similar concept at the micrometer length scale where a hemispherical cavitation bubble led to a primary and secondary fast transient jets through a holed plate. They also tested these jets for potential drug delivery applications in-vivo by using agarose gel as skin phantom. Liquid microjetting at the free surface was also achieved using optoacoustic cavitation, wherein a carbon-nano-tube (CNT) based lens was used to convert light energy of a laser into acoustic energy [14]. A cavitation bubble created inside an armoured droplet (liquid drop surrounded by solid particles) led to a plethora of jets evolving out of the armoured droplet [15].

As noted from the above literatures, the ‘bubble-bubble’ interactions can be classified as either interaction of an oscillating bubble with a stationary bubble or interaction of multiple oscillating bubbles. In the present study, we report a new kind of interaction, where an air bubble is created by the interaction of an oscillating bubble with a disturbed free surface. The interaction is somewhat similar to that reported by Pain *et al.* [9]. However, in their case, the stationary bubble was entrapped in an oil droplet before the generation of cavitation bubble close to it. In our experiments, the oscillating bubble

*badarinath@iith.ac.in

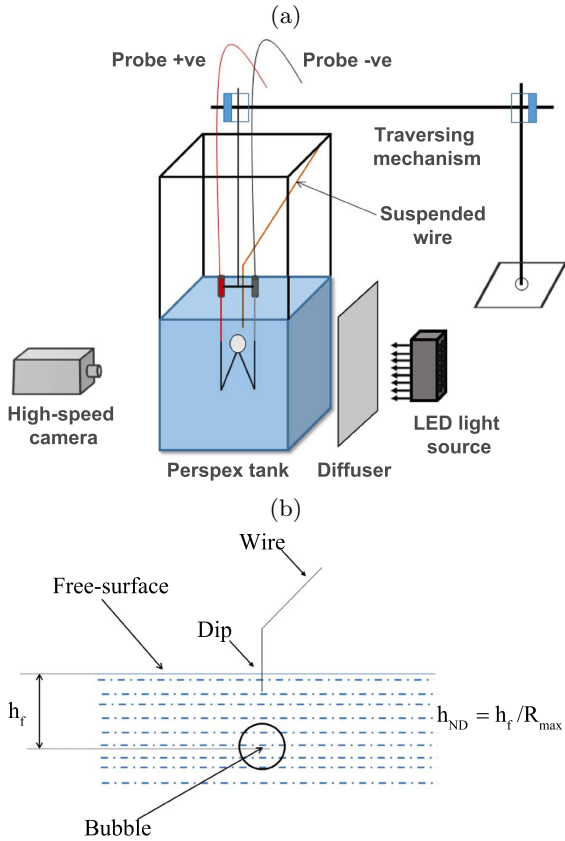


FIG. 1: (a) Schematic of the experimental set-up, and (b) illustration of various physical parameters.

itself creates a nearby air bubble. The interaction between these bubbles leads to an upward moving microjet.

Experimental set-up: The schematic of the set-up is shown in Figure 1(a). This consists of a Perspex tank (of size $450 \text{ mm} \times 450 \text{ mm} \times 450 \text{ mm}$) filled with water ($\sim 75\%$ volume). A thin wire is inserted inside water at the free surface, which forms a triple point (wire-air-water) interface with a small dip due to surface tension (shown in Figure 1(b)). A low-voltage spark circuit similar to that described by Goh *et al.* [16] is used to generate a bubble below the triple point interface. The circuit uses the principle of charging capacitors to a voltage up to 180 V through a DC power supply, and then allowing them to be short-circuited through a pair of electrodes which are placed in water. The charging, discharging and sparking circuits are connected to relays and a metal-oxide-semiconductor field-effect transistor (MOSFET), and the different parts of the circuit are controlled using NI-DAQ (model USB-6008) through a LabVIEW program.

When the capacitors are discharged through the electrodes, a cavitation bubble is created at the junction of the electrodes with R_{max} of 10.5 mm at 150 V and 12.4 mm at 180 V. The bubble pushes at the dip (at the triple point interface) while expanding and pulls at it while collapsing. Due to this push and pull of the dip, a tiny air bubble gets entrapped in water at the wire immersion

point. When the cavitation bubble collapses completely, this entrapped air bubble also collapses leading to high speed unsteady microjets at the free surface. The interaction of the entrapped air bubble with the spark generated cavitation bubble and the microjets at the free surface are recorded using a high-speed camera (Phantom V12.1, 8 bit images of 256×540 pixels, for a nominal resolution of 6 pixels/mm) with diffused back-lit illumination (LED lighting, model 900445, 12,000 lm, Visual Instrumentation Corporation). A tracing paper is used to diffuse the back light uniformly. The focal plane of the camera is always on the wire at the free surface. In order to capture the microjets, images are acquired at 20,000 frames per second (fps) with an exposure time of $10 \mu\text{s}$. Figure 1(b) shows the pictorial representation of the parameters considered in the experiments. Two different parameters are varied in the experiments: (i) the orientation of the immersed wire at the free surface, and (ii) the distance of the bubble from the triple point interface (h_f) non-dimensionalized with respect to the bubble radius ($h_{ND} \equiv h_f / R_{max}$). Note that the experiments are conducted at room temperature and atmospheric pressure. The images presented below are cropped to remove extraneous details.

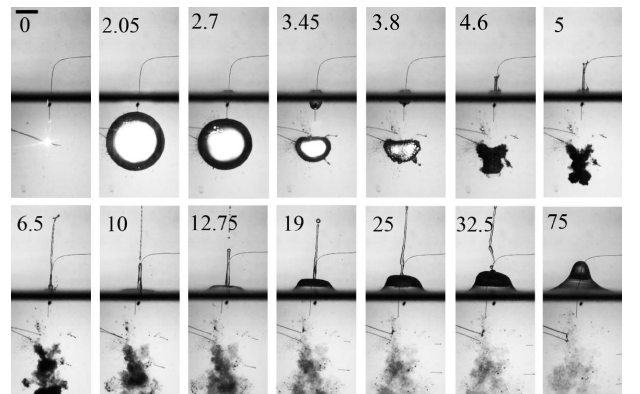


FIG. 2: Illustration of bubble dynamics and free surface microjets. Here, $R_{max} = 12 \text{ mm}$ and $h_{ND} = 1.3$. The number in each image represents the time in ms.

Discussion: Figure 2 shows a typical case to illustrate the dynamics of the formation of the entrapped bubble and high-speed jets because of the cavitation bubble. In this case, the bubble is created at $t = 0 \text{ ms}$ (sparkling time), grows to its maximum radius, R_{max} of 12 mm at $t = 2.05 \text{ ms}$ and then collapses at $t = 3.8 \text{ ms}$ with a re-entrant jet directed away from the free surface. The bubble subsequently disintegrates from $t = 3.8 \text{ ms}$ onwards as seen in the images. During the collapse phase, we can first see an entrapped bubble at $t = 2.7 \text{ ms}$ which grows and is clearly visible at $t = 3.45 \text{ ms}$. After the collapse of the spark bubble at $t = 3.8 \text{ ms}$, the entrapped bubble collapses and an initial jet as shown from $t = 5 \text{ ms}$ to about 10 ms clearly. The behaviour of the entrapped bubble can be compared with that of a ‘catapult’, wherein the entrapped bubble is undergoing expansion and contrac-

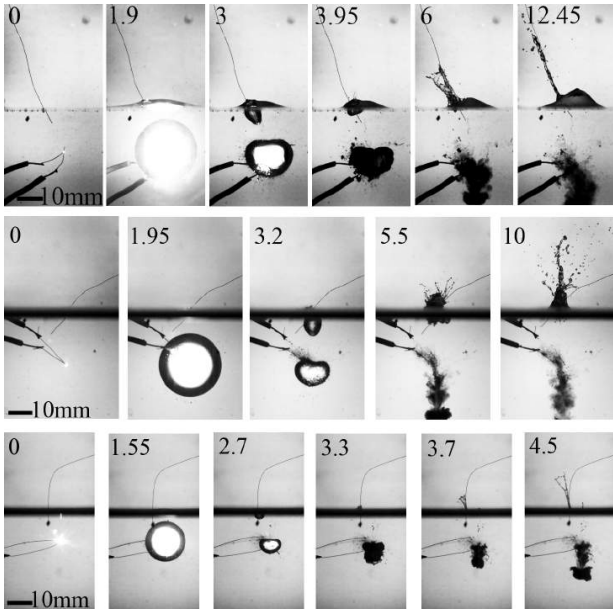


FIG. 3: Effect of wire orientation and offset on the bubble interactions and microjets. Top row: Wire is inclined and the cavitation bubble center is horizontally offset from the triple-point ($R_{max} = 11.6$ mm and $h_{ND} = 1.2$). Middle row: Wire is inclined and the cavitation bubble center is in-line with the triple point ($R_{max} = 12.2$ mm and $h_{ND} = 1.3$). Bottom row: Wire is perpendicular to the free surface and the cavitation bubble is offset from the triple point ($R_{max} = 8.6$ mm and $h_{ND} = 1.3$). The number in each image represents the time in ms.

tion due to push and pull at the dip by the cavitation bubble. Note that this jet due to the entrapped bubble first appears at $t = 4.6$ ms. At $t = 10$ ms, we notice a thin upper portion and a thick lower portion in the jet. This actually corresponds to two different jets, wherein the thick jet follows the first thin jet. From $t \approx 10$ ms to $t \approx 32.5$ ms, we see the second thick jet evolving and breaking up. The thick jet appears to be due to inertia induced in water surface by the movement of the thin jet. In this period, we also see the movement of the free surface as has been reported in an earlier study [5]. A movie showing the entire phenomenon is presented as supplementary movie 1. Supplementary movie 2 shows the top of the free surface, the dip due to the wire and the push-pull of the entrapped bubble, by recording the images at an inclined angle.

Figure 3 shows the dynamics of the entrapped bubble and free surface microjet along with the cavitation bubble under conditions when either the cavitation bubble-center is not in line with the triple-point or the wire is inclined. Four different combinations of parameters can be deduced: (a) Wire is perpendicular to the free surface and the cavitation bubble center is in-line with the triple point (Fig. 2), (b) Wire is inclined and the cavitation bubble center is horizontally offset from the triple-point (Fig. 3 top row), (c) Wire is inclined and the cava-

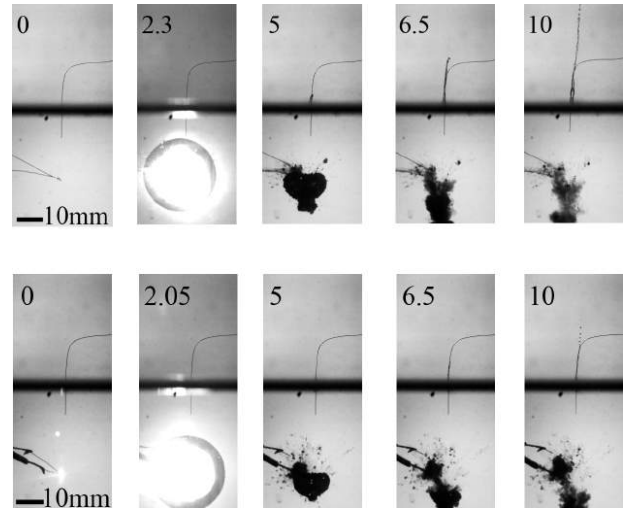


FIG. 4: Effect of $h_{ND} \equiv (h/R_{max})$ on the bubble interactions and microjets. $h_{ND} = 1.6$ (top row) and $h_{ND} = 2.1$ (bottom row) for $R_{max} = 12.2$ mm. The numbers in each image represent times in ms.

tion bubble center is in-line with the triple point (Fig. 3 middle row), and (d) Wire is perpendicular to the free surface and the cavitation bubble is offset from the triple point (Fig. 3 bottom row).

A comparison of the cases in Fig. 3 and Fig. 2 (base case) reveals that the entrapped bubble after formation always expands with its diameter along the line joining the triple-point with the center of the cavitation bubble as it expands (see Figure 3, $t = 3$ ms in top row, $t = 3.2$ ms in middle row and $t = 2.7$ ms in bottom row). When the wire is inclined or the bubble is offset, the surface microjet which forms after the entrapped bubble's collapse usually breaks up into a spray. A possible reason for this observation of break-up of jets could be that the microjet emerges from the free surface at an angle to the wire orientation unlike in the base case where the microjet emerges in the same direction as the wire orientation. This has been observed consistently across repeated experiments similar to that shown in Figure 3. Note that the bubble and the electrode cover are lying in parallel planes, but due to line-of-sight 2D visualisation, it gives an impression that they are in contact (see Fig. 3 top row) while it is not actually so. We also observed through several experiments that the orientation of the electrode cover does not effect the bubble dynamics.

The effect of varying the non-dimensional distance (h_{ND}) on the entrapped bubble and the microjet formation is presented in Figure 4 for two values of h_{ND} , namely, $h_{ND} = 1.6$ (top row) and $h_{ND} = 2.1$ (bottom row). In both the cases, the maximum bubble radius, R_{max} is fixed at 12.2 mm. A comparison of the top and bottom panels reveals that as h_{ND} increases, the movement of the dip on the free surface decreases. This in turn is reflected in a smaller entrapped bubble and a less energetic jet (see frames corresponding to the same time).

It should be noted here that as the h_{ND} is further increased, a limiting h_{ND} of 2.6 is observed beyond which there is no effect of the cavitation bubble in forming an entrapped bubble. This limiting h_{ND} is also observed to be independent of the bubble radius (voltage) over R_{max} values range from 3.5 to 12.4 mm.

To summarise, the phenomenon of the formation of an entrapped air bubble and two microjets because of the creation of a cavitation bubble below a free surface is reported. When a wire is placed on the free surface creating a triple point (wire-water-air) interface and a cavitation bubble is created below it, then there is entrapment of an air bubble due to the expansion and collapse of the cavitation bubble resembling a ‘catapult’ effect. To the best of our knowledge, this behaviour has been reported for the first time in the present study. After the collapse of the cavitation bubble, the entrapped air bubble also collapses leading to two microjets on the free surface. The effect of the inclination of the wire and the non-

dimensional distance of the bubble from the free surface (h_{ND}) on the dynamics of the entrapped air bubble and the microjets are studied. An inclined wire leads to the formation of a spray, which is not observed in case of a wire placed perpendicular to the free surface. As h_{ND} increases, the strength of the ‘catapult’ effect and the microjets decreases, eventually leading to a limiting h_{ND} , for which no bubble entrapment takes place.

Supplementary Material: Supplementary movie 1 illustrates bubble dynamics and formation of free surface microjets. Supplementary movie 2 shows the top of the free surface, the dip due to the wire and the push-pull of the entrapped bubble, by recording the images at an inclined angle. The parameters are the same as those used in Figure 2.

Acknowledgment: KB would like to acknowledge the Science and Engineering Research Board (SERB), Department of Science and Technology (DST) India for their financial support through the project grant No. ECR/2015/000311.

-
- [1] G. L. Chahine, “Interaction between an oscillating bubble and a free surface,” *Trans. ASME J. Fluids Engg.* **99**, 709 (1977).
- [2] J. R. Blake and D. C. Gibson, “Growth and collapse of a vapour cavity near a free surface,” *J. Fluid Mech.* **111**, 124 (1981).
- [3] M. S. Plesset and R. B. Chapman, “Collapse of an initially spherical vapour cavity in the neighbourhood of a solid boundary,” *J. Fluid Mech.* **47**, 283 (1971).
- [4] S. C. Kian and A. C. Junior, “Fluid needles: Transforming shock waves into syringes,” *Proc. of Nanyang Research Programme* (2009).
- [5] S. Zhang, S. P. Wang and A. M. Zhang, “Experimental study on the interaction between bubble and free surface using a high-voltage spark generator,” *Phys. Fluids* **28**, 032109 (2016).
- [6] Y. Tagawa, N. Oudalov, C. Visser, I. R. Peters, D. van der Meer, C. Sun, A. Prosperetti, and D. Lohse, “Highly focused supersonic microjets,” *Phys. Fluids Dynamics* **2**, 31002 (2012).
- [7] J. R. Blake, P. B. Robinson, A. Shima and Y. Tomita, “Interaction of two cavitation bubbles with a rigid boundary,” *J. Fluid Mech.* **255**, 707 (1993).
- [8] K. Jungnickel and A. Vogel “Interaction of two laser-induced cavitation bubbles,” In: Blake J.R., Boulton-Stone J.M., Thomas N.H. (eds) *Bubble Dynamics and Interface Phenomena. Fluid Mechanics and Its Applications* **23**, 47 (1994).
- [9] A. Pain, B. H. T. Goh, E. Klaseboer, S. -W. Ohl and B. C. Khoo, “Jets in quiescent bubbles caused by a nearby oscillating bubble,” *J. of Appl. Phys.* **111**, 054912 (2012).
- [10] S. W. Fong, D. Adhikari, E. Klaseboer and B. C. Khoo, “Interactions of multiple spark-generated bubbles with phase differences,” *Exp. in fluids* **46**, 705 (2009).
- [11] B. Karri, S. R. Gonzalez-Avila, Y. C. Loke, S. J. O’Shea, E. Klaseboer, B. C. Khoo and C. -D. Ohl, “High-speed jetting and spray formation from bubble collapse,” *Phys. Rev. E* **85**, 015303 (2012).
- [12] B. Karri, S. -W. Ohl, E. Klaseboer, C. -D. Ohl and B. C. Khoo, “Jets and sprays arising from a spark-induced oscillating bubble near a plate with a hole,” *Phys. Rev. E* **86**, 036309 (2012).
- [13] S. R. G. Avila, C. Song and C. -D. Ohl, “Fast transient microjets induced by hemispherical cavitation bubbles,” *J. Fluid Mech.* **767**, 31 (2015).
- [14] T. Lee, H. W. Baac, J. G. Ok, H. S. Youn, and L. J. Guo, “Nozzle-free liquid microjetting via homogeneous bubble nucleation,” *Phys. Rev. App.* **3**, 44007 (2015).
- [15] J. O. Marston and S. T. Thoroddsen, “Laser-induced micro-jetting from armored droplets,” *Exp. in Fluids.* **56**, 140 (2015).
- [16] B. H. T. Goh, Y. D. A. Oh, E. Klaseboer, S. -W. Ohl and B. C. Khoo, “A low-voltage spark-discharge method for generation of consistent oscillating bubbles,” *Rev. Sci. Instru.* **84**, 014705 (2013).